SAE International™

Links between Notchback Geometry, Aerodynamic Drag, Flow Asymmetry and Unsteady Wake Structure

2011-01-0166
Published
04/12/2011

David Sims-Williams, David Marwood and Adam Sprot
Durham University

doi:10.4271/2011-01-0166

ABSTRACT

The rear end geometry of road vehicles has a significant impact on aerodynamic drag and hence on energy consumption. Notchback (sedan) geometries can produce a particularly complex flow structure which can include substantial flow asymmetry. However, the interrelation between rear end geometry, flow asymmetry and aerodynamic drag has lacked previous published systematic investigation.

This work examines notchback flows using a family of 16 parametric idealized models. A range of techniques are employed including surface flow visualization, force measurement, multi-hole probe measurements in the wake, PIV over the backlight and trunk deck and CFD.

It is shown that, for the range of notchback geometries investigated here, a simple offset applied to the effective backlight angle can collapse the drag coefficient onto the drag vs backlight angle curve of fastback geometries. This is because even small notch depth angles are important for a sharp-edged body but substantially increasing the notch depth had little further impact on drag.

This work shows that asymmetry originates in the region on the backlight and trunk deck and occurs progressively with increasing notch depth, provided that the flow reattaches on the trunk deck and that the effective backlight angle is several degrees below its crucial value for non-reattachment. A tentative mapping of the flow structures to be expected for different geometries is presented.

CFD made it possible to identify a link between flow asymmetry and unsteadiness. Unsteadiness levels and principal frequencies in the wake were found to be similar to those for high-drag fastback geometries. The shedding of unsteady transverse vortices from the backlight recirculation region has been observed.

INTRODUCTION

As is well known, the rear end geometry of road vehicles can have the greatest influence on aerodynamic drag coefficient and hence on energy consumption for highway driving. Understanding of the link between rear end geometry, flow structure and drag is therefore of central importance. Of the three classical rear end geometries (square-back, fastback, notchback), the complex flow structure behind the notchback, (three box / sedan / saloon) has been the least well understood.

Notchbacks, like fastbacks, exhibit a maximum drag associated with strong trailing vortices from the c-pillars and this occurs when the time-averaged flow separates over the backlight but reattaches just before the rear of the vehicle. For notchbacks the effective (or apparent) backlight angle has been used as the geometry parameter for characterizing when the flow will transition from this maximum drag condition to a fully separated (and lower drag) rear end flow. Figure 1 illustrates the backlight angle (B) and effective backlight angle (B_{eff}) for a notchback. Nouzawa et al [1] found that the drag coefficient changes with rear end geometry were less extreme for notchbacks than for fastbacks. It should be noted that the effective backlight angle is far from being a perfect index to rear end flow structure, with critical effective backlight angles varying significantly between different notchback geometries (eg: [1] vs [2]). This is further

illustrated by Howell [3] (summarizing unpublished work by Windsor) which shows that the use of effective backlight angle cannot collapse the drag of different notchback geometries. Improving on the effective backlight parameter for the classification of a wider range of notchback geometries is one of the aims of the present work.

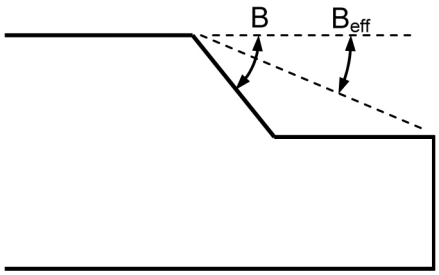

Figure 1. Definition of Effective Backlight Angle

Perhaps the most intriguing aspect of notchback rear end flows is the common presence of an asymmetric rear end flow for symmetric geometries. Gaylard et al [4] compiled a number of cases (eg: [5], [6], [7], [8], [9]) in which asymmetry has been observed in the wake structure of notchback vehicle types, including real vehicles and idealized geometries. In most cases these observations were anecdotal to the subject of the original investigation. Gaylard et al [4] highlighted that further work was required to understand the effects of different notchback geometries. Additionally, it remains unclear what the effects of asymmetry are, if any, on the lift and drag performance of the vehicle. The link between notchback geometry and asymmetry has lacked previous systematic investigation and this will be one of the aims of this work.

Notchbacks, like other road vehicles, have rear end flows dominated by significant flow separation, which in turn leads to significant flow unsteadiness. Gilhome et al [10] have proposed an unsteady flow topology for notchbacks and this will be investigated for the geometry used here. Some detailed flow structure measurements were made for a notchback by Jenkins [11] however, these were confined to a geometry with a symmetric flow structure and so this work will focus, in particular, on the case of asymmetric flow.

This work seeks to achieve the following objectives:

• To assess how wake structure, including in particular any asymmetry, depends on notchback geometry.

• To assess the dependence of the drag of a notchback on rear end geometry (including noting any links with asymmetry).

• To provide a clearer understanding of the time-averaged wake structure behind a notchback.

• To investigate the unsteady nature of the wake behind a notchback, including identifying Strouhal numbers and testing the unsteady topology put forward by Gilhome et al [10].

APPROACH

Wind tunnel tests and CFD simulations were performed using a family of basic geometries. The front end geometry of Ahmed et al [12] was adopted as this provides a clean flow onto the rear of the model and avoids the presence of artifacts from the front end flow (eg: A-pillar vortices) confusing observations of the rear end flow or introducing geometry-specific interactions.

The experimental phase of the work used 16 interchangeable rear end geometries assembled from machined Aluminum tooling plate for the purpose of this study. Geometries were selected to provide effective backlight angles including reattaching and separated flows and backlight angles ranging from fastback to 90° while maintaining constant trunk deck height and model length. The aim here was to capture symmetric and asymmetric as well as high and low drag flow structures. The models were nominally equivalent to 25% scale, as used by [12]. Testing was in the Durham University 2 m^2 open jet wind tunnel in fixed ground configuration (described in [13], [14]); the resulting cross sectional area blockage was 5.6%. The Reynolds number, based on model length, was 1.9×10^6.

A subset of the geometries were simulated using Ansys Fluent (version 6.3). The simulations were performed at the same Reynolds number as the experiments but with a larger computational domain (0.4% blockage with inlet and outlet both 16 model lengths away from the model). Following a study of turbulence model and grid-independence, the Spallart-Almeras turbulence model was used with a structured mesh of approximately 1.2×10^6 cells, corresponding to y+ values between 25 and 75. Both steady and time resolved simulations were performed, the latter with a time step of 0.005 s and simulation time of 2.5 s.

RESULTS

SURFACE FLOW VISUALIZATION - ASSESSMENT OF ASYMMETRY

Surface flow visualization was performed for all of the models in order to assess asymmetry in the rear end flow. This was done using fluorescent toner mixed with paraffin, with UV lighting to better view the resulting patterns. Ink drop flow observations were used to confirm flow directions wherever this was unclear.

The flows can be divided into three classifications: Fully Separated, Reattaching Symmetric, and Reattaching Asymmetric. For the steepest effective backlight angles the flow was clearly fully separated over the entire backlight and

trunk deck; there was no evidence of asymmetry in any of these cases. For low effective backlight angles the flow separated at the sharp top of the backlight but reattached on the backlight itself (for the lowest backlight angles) or on the trunk deck. For some geometries this reattaching flow was symmetric while for others it exhibited different levels of asymmetry. Where possible, critical points are identified. Figure 2 illustrates a reattaching symmetric flow while Figure 3 illustrates a strongly asymmetric reattaching flow. The range of levels of asymmetry that were observed seems to indicate that the asymmetry develops progressively rather than being a fundamental change in the flow topology.

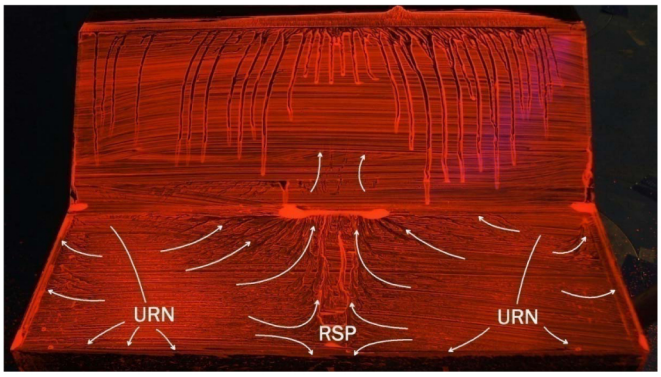

Figure 2. Surface Flow - Symmetric Reattaching (B_{eff} = 21°, B = 42°)

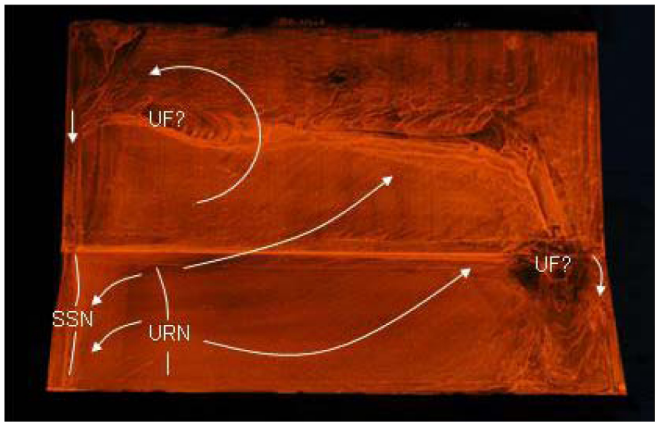

Figure 3. Surface Flow - Reattaching Asymmetric (B_{eff} = 17.8°, B = 31.8°)

FORCE MEASUREMENTS

Aerodynamic forces were recorded for all 16 geometries. Forces were corrected according to [15], the correction on the coefficients in this case is about 1%. The total repeatability in this facility is 0.002 on C_D.

Figure 4 presents the measured drag coefficient plotted against the effective backlight angle and Figure 5 illustrates the rear lift coefficient. Reattaching and fully separated cases are labeled based on the surface flow visualization. As expected, at relatively low effective backlight angles the drag increases as effective backlight angle increases up to a maximum drag condition. This corresponds to a flow which is separated over the backlight and trunk deck but which reattaches just before the end of the trunk deck. When the effective backlight angle exceeds 25°–30° the flow separates without reattachment and once this condition is reached the drag is reduced to essentially the same value as for a squareback. The rear lift coefficient (defined in this case based on the lift at the rear mounting legs) also increases with increasing effective backlight angle for the reattaching flows and then drops to a lower and more universal level for the fully separated cases.

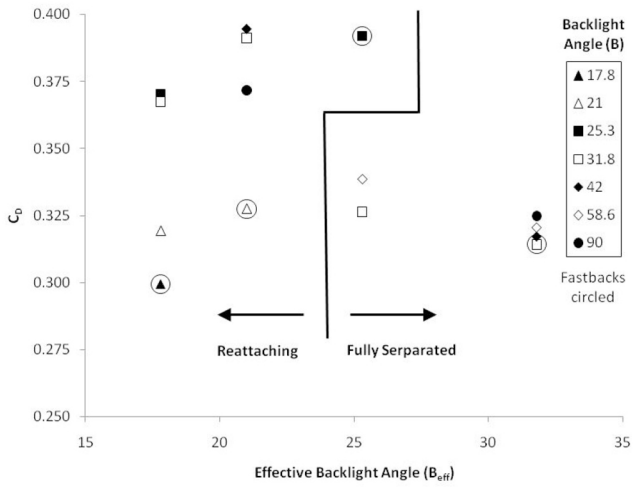

Figure 4. Drag and Flow Structure Dependence on Effective Backlight Angle

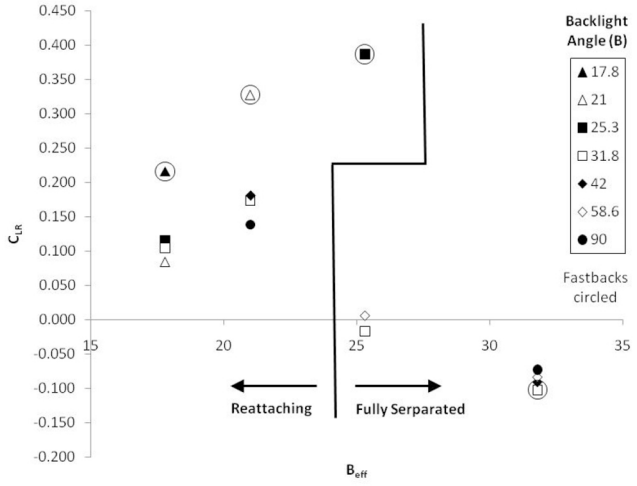

Figure 5. Rear Lift Dependence on Effective Backlight Angle

While the effective backlight angle is a good first parameter for characterizing the flow over a notchback geometry it is obviously not the only important parameter. The notch depth angle ($B - B_{eff}$) is proposed as a useful second parameter which quantifies the amount by which a notchback differs from a fastback of equivalent effective backlight angle. For a given effective backlight angle, increasing notch depth angle will move the flow towards the fully separated condition. If the flow remains reattaching then a steeper actual backlight angle will usually increase drag but if it provokes full separation then it will decrease drag.

For a sharp edged geometry as investigated here, notch depth angles of as little as 3 degrees have a measureable effect. However, the maximum impact of the notch depth on the drag or flow structure at a given effective backlight angle was limited (for example, Figure 4, B_{eff}=17.8°, B increasing from 17.8° up to 25.3° produced a effect but further increasing B had no further effect). Figure 6 illustrates that simply adding 3.5 degrees to the effective backlight angle to represent the effect of the presence of the notch provides a significant collapse of the data of Figure 4 onto a single curve encompassing both fastbacks and notchbacks, including those with backlight angles ranging up to 90°. It should be noted that, while the collapse of C_D data seems quite good, the same approach does not simultaneously collapse rear lift data. This is partly because different geometries will have different horizontal projected areas for the combined backlight and trunk lid where the vertical projected areas, on which drag largely depends, are constant. This approach is presented to show the relatively simple (ie: binary) impact of notch depth angle for this family of sharp edged geometries, rather than to attempt to provide a universal parameter for all notchback geometries.

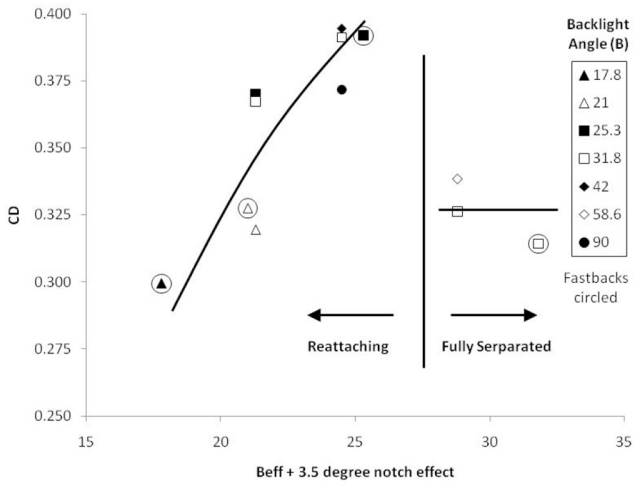

Figure 6. Collapse of Drag Using 3.5° Notch Effect

While reattaching and fully separated flow structures can be clearly identified in the force data, asymmetric cases are inconspicuous. Figure 7 tentatively illustrates which of the three fundamental flow structures will be present (fully separated, reattaching symmetric or reattaching asymmetric) for a wide range of configurations. The bottom edge of the plot corresponds to fastback geometries (zero notch depth angle). Contours of drag coefficient are superimposed in Figure 7 while Figure 8 includes contours of rear lift coefficient. The contour values need to be treated as illustrative as they are based on a relatively small number of discrete points. The actual test geometries used in this study are identified on the plots.

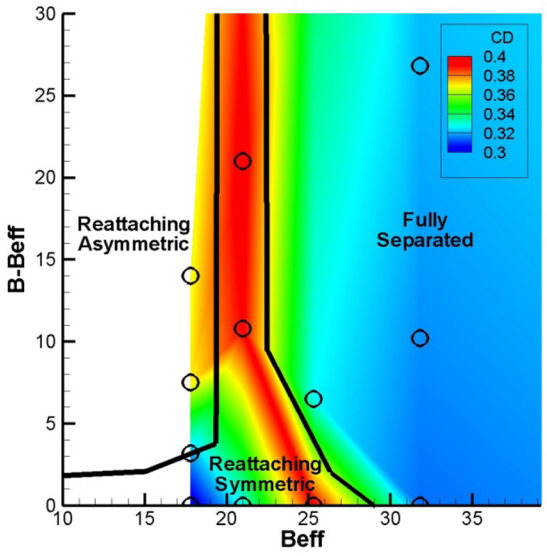

Figure 7. Drag and Flow Structure Dependence on Backlight Geometry

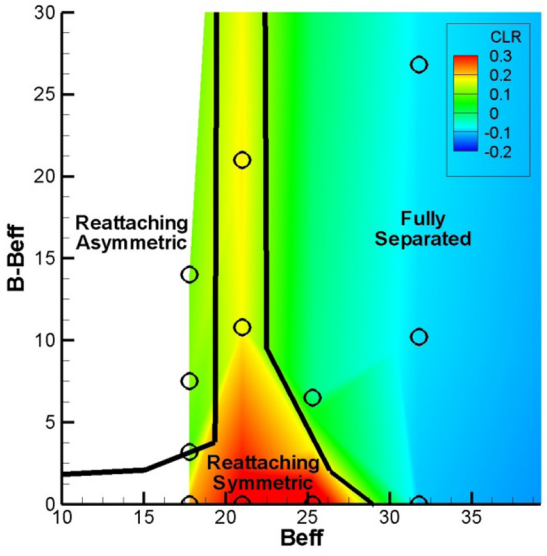

Figure 8. Rear Lift and Flow Structure Dependence on Backlight Geometry

The effect of notch depth angle (B - B_{eff}) on critical effective backlight angle can be seen. Notch depth angles of a few degrees provide an effect equivalent to a few degrees of effective backlight angle. However, further increases in notch depth angle provide little additional effect, even when notch depth angle is large (>20°).

Figure 7 and Figure 8 also map the geometries which lead to asymmetric reattaching flows. Asymmetric flows occur specifically for notchback geometries but not for fastbacks and the level of asymmetry increases with notch depth angle. For example: for an effective backlight angle of 17.8° a notch depth angle of 3.2° results in relatively mild asymmetry. When the notch depth angle is increased to 6.5° (at the same effective backlight angle) the flow becomes fully asymmetric. However, asymmetric flows seem not to occur for cases very close to the maximum drag condition, irrespective of how extreme notch depth angle becomes. Even notch depth angles approaching 70° did not cause asymmetry when the flow was close to critical backlight angle. This is consistent with Jenkins [11] who saw no asymmetry even with a vertical backlight. The presence of asymmetry on production notchbacks should not therefore be surprising, since it seems likely to occur for even mild notch depth angles when the effective backlight angle is safely below the high drag condition (as would be the aim in a production vehicle).

FLOW FIELD - TIME AVERAGED

Flow field data were measured using a 5-hole probe calibrated over a pitch and yaw range extending to ±60°. Transfer function correction for tubing distortion was applied (as described and validated in [16] and [17] respectively) to allow accurate time-resolved measurements. The data was sampled at 1000 Hz and was low pass filtered at 250 Hz, the probe itself could achieve a frequency response up to 1000 Hz.

Particle image velocimetry (PIV) was used above the trunk lid and backlight where reversed flow dominates. The system employed an ILA synchonizer, Sensicam 12 bit, 1280×1024 camera with chip cooling and a New Wave Research 120mJ double headed Nd: YAG laser. The flow was seeded with 1µm droplets of di-ethylhexyl sebacate (DEHS) using a compressed air fed, 40 nozzle atomizer. The seeding was injected into the airflow in a single pass by means of a smoke rake positioned upstream of the nozzle contraction where it provided minimal disruption to the airflow upstream of the model. For each measurement plane 1000 image pairs were collected.

Flow field measurements were made for a selection of geometries including examples of symmetric and asymmetric reattaching flows and fully separated flow. Of greatest interest is the reattaching asymmetric flow and therefore that will be the focus of the work presented here; the specific case presented is an effective backlight angle of 17.8° and backlight angle of 31.8° (notch depth angle = 14°). The case presented corresponds to the surface flow visualization of Figure 3. Figure 9 provides an overview of the flow-field, combining data from PIV over the backlight with probe data. This is consistent with the surface flow visualization with the divide between the two trailing vortex structures aligned with the URN labeled on the trunk deck in Figure 3.

Asymmetry in the separation over the backlight is clear, as is the asymmetry in the loss core of the trailing vortices. However, there is no indication of a radically different flow structure to the familiar symmetric case present for fastback geometries. The asymmetry in the size of the backlight separation translates into asymmetry in the trailing vortices and this asymmetry propagates downstream.

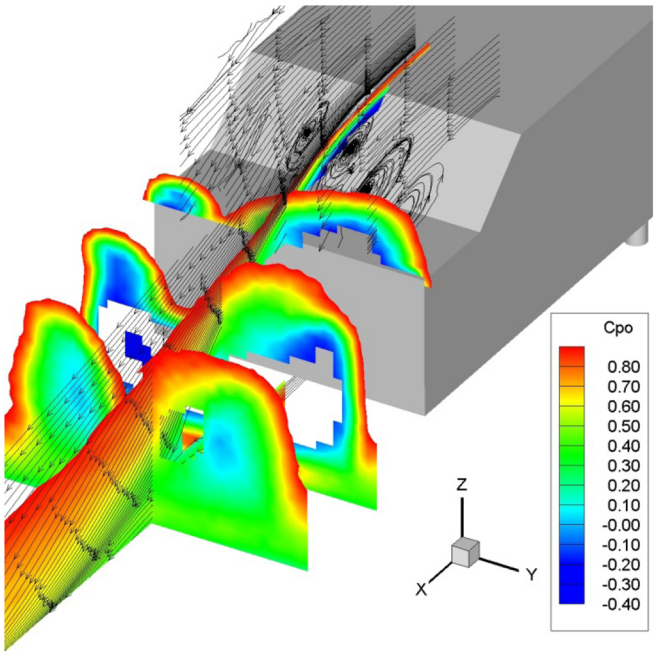

Figure 9. Asymmetric Reattaching Flow Overview of Probe and PIV Measurements (B_{eff} = 17.8°, B = 31.8°)

The concept that notchback asymmetric flows are incremental rather than transformative fits with the observations of a progressive asymmetry with increasing notch depth angle discussed earlier, and with observations made by Gaylard et al [4], that notchback asymmetry can be an asymmetric version of the same fundamental flow structure seen in symmetric cases.

Figure 11 illustrates time-averaged PIV vectors on the centerline above the backlight and trunk deck for the same geometry. Figure 10 and Figure 12 illustrate corresponding vectors on either side of the centerline. All three figures show straightforward separation originating at the top of the backlight and reattaching near the rear of the trunk deck. As

can also be seen in Figure 9, the size of the recirculation region is smaller for planes to the left of the centerline and is larger for planes to the right, however in all cases the PIV confirms that the flow reattaches before the end of the trunk deck. It is important to remember that the PIV data illustrates only in-plane velocity components whereas the surface flow visualization of Figure 3 shows significant transverse flow. PIV measurements even further to the left, at y/W = −.33, showed no recirculation and it is postulated that a vortex terminates on the backlight in this region (the left hand UF in Figure 3). This vortex partially resembles the arch vortex proposed by Nouzawa et al [1] except that that work showed the ends of the vortex terminating entirely on the trunk lid on both sides. Figure 3 indicates that it terminates principally on the backlight on the left hand side and the combined observations made here suggest that it terminates at the front of the trunk deck on the right hand side.

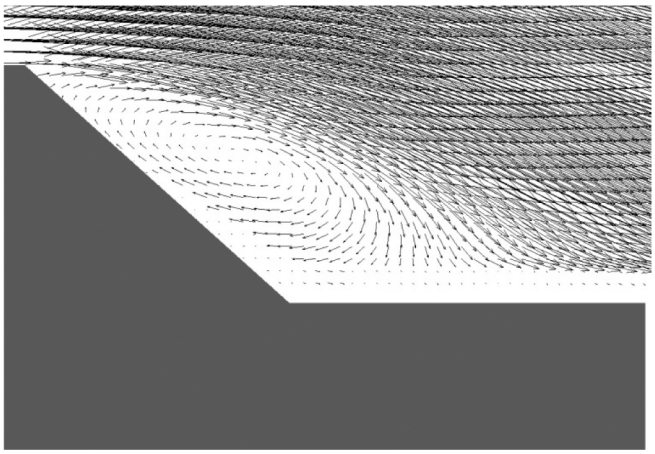

Figure 10. PIV Vectors at y/W = −0.17 (Asymmetric Reattaching Flow, B_{eff} = 17.8°, B = 31.8°)

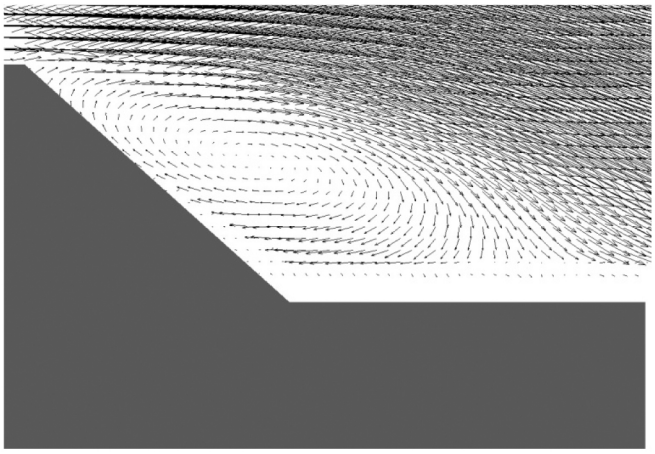

Figure 11. PIV Vectors on Centerline (Asymmetric Reattaching Flow, B_{eff} = 17.8°, B = 31.8°)

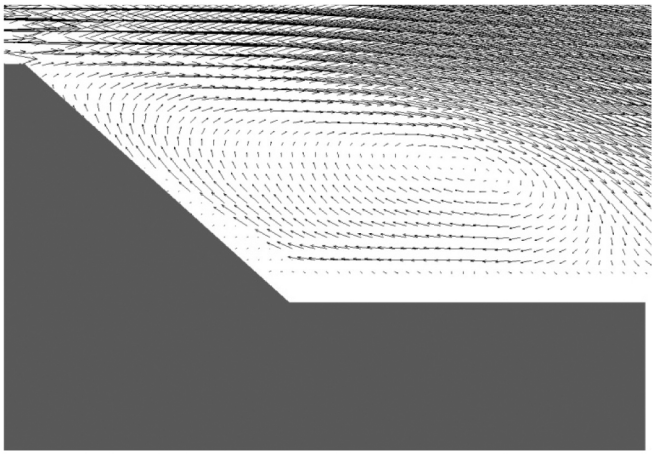

Figure 12. PIV Vectors at y/W = +0.17 (Asymmetric Reattaching Flow, B_{eff} = 17.8°, B = 31.8°)

UNSTEADINESS

The notchback wake was found to exhibit similar levels of unsteadiness to that measured previously for fastbacks (eg: [18], [19]). Figure 13 illustrates the level of total velocity fluctuation, non-dimensionalised by free stream velocity, measured at a plane at x/sqrt(A) =1.0 behind the model. This is the most downstream of the three cross planes visible in Figure 9. As for fastbacks, the unsteadiness is concentrated around the periphery of the trailing vortices and downstream of the under-floor region. Sims-Williams and Duncan [19] found a dominant frequency corresponding to a Strouhal number of approximately 0.5 for the Ahmed model in a high drag condition and demonstrated the unsteady structure responsible. In the present case similar frequencies are observed (principal Stouhal numbers in different regions are included on Figure 13) but the unsteadiness appears less coherent over the wake.

Strouhal number is defined as:

$$S = \frac{f\sqrt{A}}{U} \qquad (1)$$

Where f is frequency, A is model frontal area and U is free stream velocity.

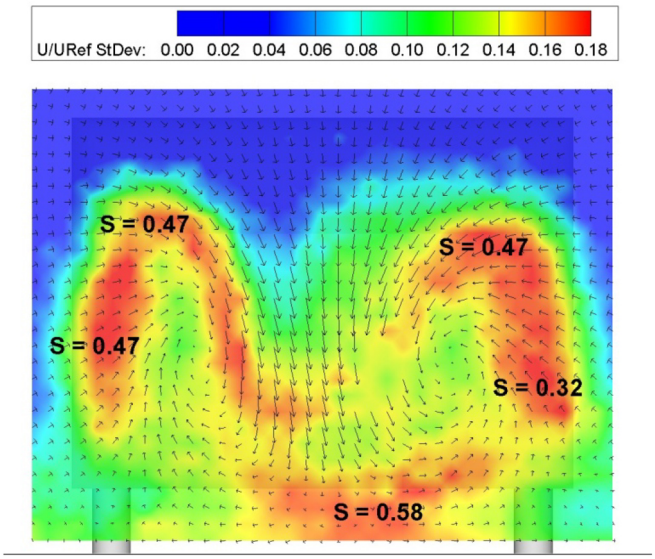

Figure 13. Velocity Fluctuation at x/sqrt(A) = 1.0 (from 5 Hole Probe) (B_{eff} = 17.8°, B = 31.8°)

The potential importance of unsteadiness to the notchback flow structure, and to asymmetry in particular, was investigated by performing steady state and time-resolved CFD simulations. While steady-state simulations were able to predict the flow structures for symmetric reattaching and fully separated geometries they failed to predict asymmetric flow structures. Performing an unsteady calculation, with a time-step designed to resolve unsteadiness up to the primary frequencies seen in Figure 13, made it possible to correctly predict both symmetric and asymmetric flows for the relevant geometries, as illustrated in Figure 14 and Figure 15.

Gilhome et al [10], considering symmetric flows over notchbacks, proposed an unsteady structure over the backlight and trunk deck involving the unsteady shedding of "hairpin" vortices from the periphery of the backlight recirculation region. Gilhome et al observed Strouhal numbers (based on reattachment length) of 0.11 and 0.42. These frequencies would approximately correspond to Strouhal numbers of 0.3 and 1.2 based on square root of model frontal area in this case, the former being similar to values identified in Figure 13.

The PIV post-processing technique of Konstantinidis et al [20] was implemented in order to seek out repeating flow structures. This involves calculating cross-correlations between all individual instantaneous PIV vector fields and then averaging groups of fields which are closely correlated in the region of interest. This provides some noise rejection and data reduction compared with examining instantaneous fields. Figure 16 and Figure 17 illustrate conditional averages of a few instantaneous PIV captures each and show a tightening and opening of the recirculation region over the backlight on the centerline, compared with the average vector field presented in Figure 11. These share some similarities with the sketches of Gilhome et al [10], reproduced here as Figure 18.

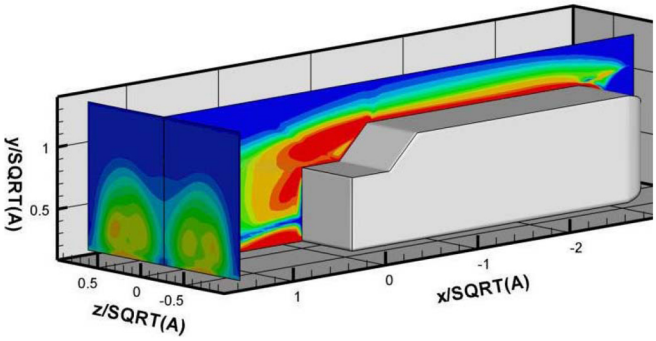

Figure 14. CFD Contours of Total Vorticity Magnitude for Symmetric Case (B_{eff} = 21.0°, B = 42.0 °)

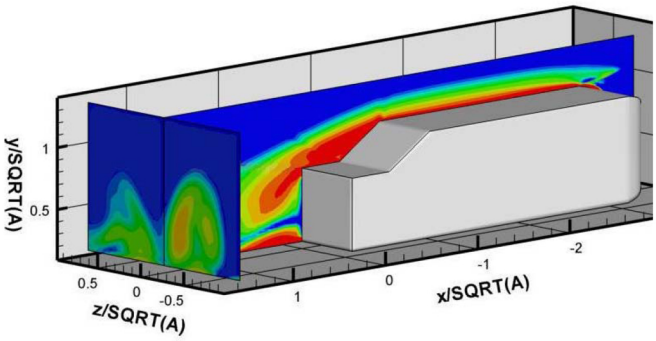

Figure 15. CFD Contours of Total Vorticity Magnitude for Asymmetric Case (B_{eff} = 17.8°, B = 31.8°)

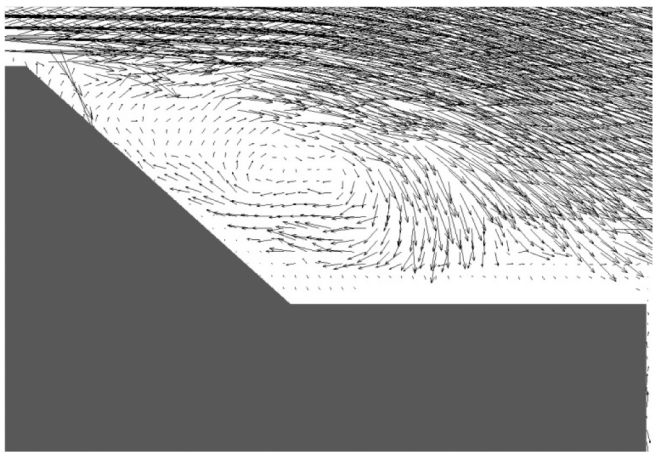

Figure 16. Correlated PIV Vector Field on Centreline #1 (B_{eff} = 17.8°, B = 31.8°)

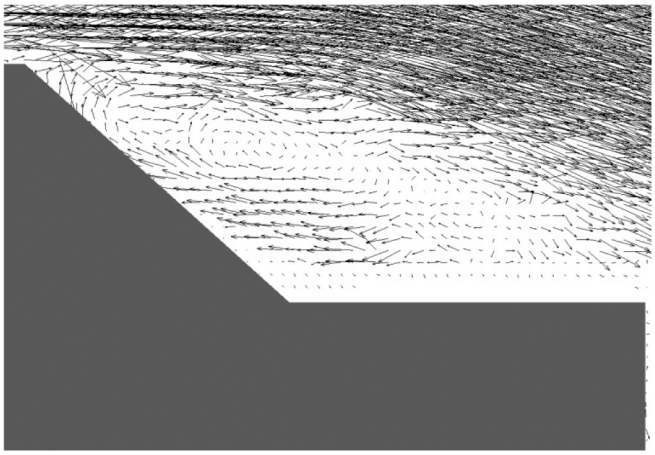

Figure 17. Correlated PIV Vector Field on Centreline #2 (B_{eff} = 17.8°, B = 31.8°)

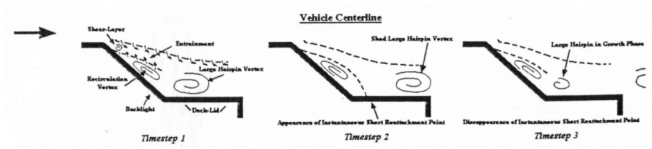

Figure 18. Proposed Notchback Centerline Flow from [10]

Examining transverse vorticity in the PIV vector fields shows that the shear (vorticity) is strongest at the periphery of the recirculation, the flow inside the recirculation possessing very little energy. This is illustrated in the time-averaged vorticity on the centerline over the backlight presented in Figure 19. When instantaneous, or conditionally averaged, fields are examined (Figure 20) it is possible to observe distinct vortices within the shear layer. These will be the source of the majority of the transverse vorticity that is shed into the model wake. The passing frequency of the vorticity packets visible in Figure 20 was calculated from their nominal physical separation and the local velocity (approximately 65% of the free stream velocity) and this is illustrated on the figure. This analysis shows that the frequency associated with unsteadiness within the shear layer is about an order of magnitude above the frequencies that propagate into the wake.

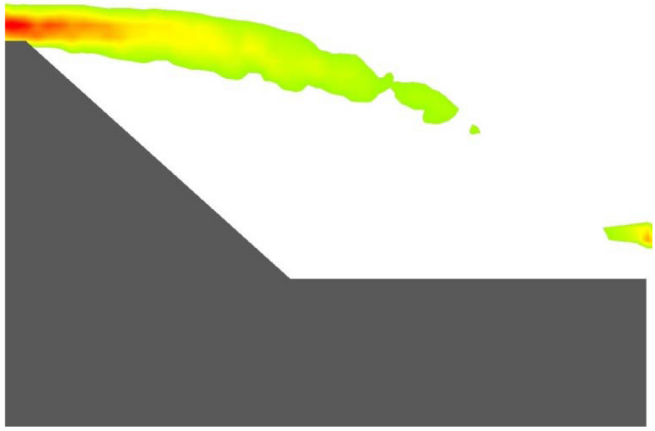

Figure 19. Clockwise Vorticity on Centerline - Time-Averaged PIV (B_{eff} = 17.8°, B = 31.8°)

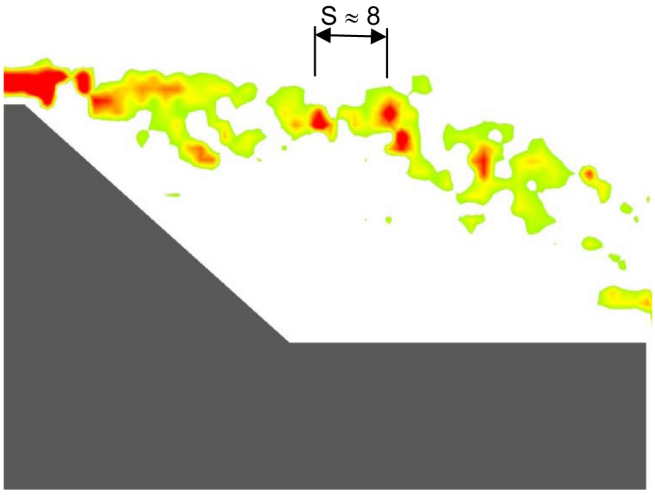

Figure 20. Clockwise Vorticify on Centerline for Correlated PIV Vector Field (B_{eff} = 17.8°, B = 31.8°)

CONCLUSIONS

Links between notchback rear end geometry, flow structure and forces have been identified. It has been shown for the family of geometries considered here that a simple offset applied to the effective backlight angle can collapse the drag coefficient for different notchback geometries onto the drag vs backlight angle characteristic of fastback geometries. This is because even small notch depth angles are important for a sharp-edged body but increasing the notch depth had little further impact on drag.

The link between notchback geometry and asymmetry has been explored and it has been shown that asymmetry occurs for increased notch depth angle for reattaching flows at effective backlight angles several degrees below the critical angle. A tentative mapping of the flow structures to be expected for different geometries is presented. While

asymmetry was not seen to affect drag, it could be an indicator of a rear end design which is safely away from a maximum drag geometry.

Asymmetry can be seen to originate with an asymmetric recirculation region on the backlight and trunk deck of the model and this in turn results in an asymmetric wake. The flow structure elements in the asymmetric case appear to be the same as those for symmetric cases.

Unsteadiness levels in the wake are similar to those for high-drag fastback geometries and Strouhal numbers in the region of 0.4 were observed which is similar to those for fastbacks. Unsteadiness in the shedding of transverse vorticity from the backlight recirculation region has been observed (at S~8) and this could be consistent with the unsteady structure proposed by Gilhome et al [10].

REFERENCES

1. Nouzawa, T., Haruna, S., Hiasa, K., Nakamura, T. et al., "Analysis of Wake Pattern for Reducing Aerodynamic Drag of Notchback Model," SAE Technical Paper 900318, 1990, doi: 10.4271/900318.

2. Carr, G., "Influence of Rear Body Shapes on the Aerodynamic Characteristics of Saloon Car" MIRA Report Number 1974/2 1974.

3. Howell, J., "Shape and Drag" Euromotor Short Course Using aerodynamics to Improve the Properties of Cars, Stuttgart, February, 1998.

4. Gaylard, A.P., Howell, J.P., and Garry, K.P., "Observation of Flow Asymmetry Over the Rear of Notchback Vehicles," SAE Technical Paper 2007-01-0900, *SAE Transactions - Journal of Passenger Cars: Mechanical Systems*, 2007, doi: 10.4271/2007-01-0900.

5. Cogotti, A., "Car-Wake Imaging Using a Seven-Hole Probe," SAE Technical Paper 860214, 1986, doi: 10.4271/860214.

6. Hetherington, B. and Sims-Williams, D. "Support Strut Interference Effects on Passenger and Racing Car Wind Tunnel Models," SAE Technical Paper 2006-01-0565, 2006, doi:10.4271/2006-01-0565.

7. Lawson, N., Garry, K.Faucompret, N., "An Investigation of the Flow Characteristics in the Bootdeck Region of a Scale Model Notchback Saloon Vehicle" *Proceedings of the Institution of Mechanical Engineers, Part D: Journal of Automotive Engineering* 221(6):739-754, 2007.

8. Cogotti, A., "Recent Advances in Flow Field Mapping Techniques," SAE Technical Paper 870718, 1987, doi: 10.4271/870718.

9. Garry, K.P., Le Good, G.M., "An Investigation of the Sensitivity of Rear Wing Orientation for Saloon Race Cars," SAE Technical Paper 2005-01-1018, 2005, doi: 10.4271/2005-01-1018.

10. Gilhome, B.R., Saunders, J.W., and Sheridan, J., "Time Averaged and Unsteady Near-Wake Analysis of Cars," SAE Technical Paper 2001-01-1040, 2001, doi: 10.4271/2001-01-1040.

11. Jenkins, L.N., "An Experimental Investigation of the Flow Over the Rear End of a Notchback Automobile Configuration," SAE Technical Paper 2000-01-0489, 2000, doi:10.4271/2000-01-0489.

12. Ahmed, S.R., Ramm, G., and Faltin, G., "Some Salient Features of The Time-Averaged Ground Vehicle Wake," SAE Technical Paper 840300, 1984, doi: 10.4271/840300.

13. Sims-Williams, D.B. and Dominy, R.G., "The Design of an Open-Jet Wind Tunnel for Model Testing," SAE Technical Paper 2002-01-3340, 2002, doi: 10.4271/2002-01-3340.

14. Sims-Williams, D.Dominy, R., "The Design of a New Wind Tunnel for Vehicle Aerodynamics Research" MIRA Vehicle Aerodynamics Conference, Warwick, UK, 2002.

15. SAE, "Aerodynamic Testing of Road Vehicles in Open Jet Wind Tunnels," SAE International, Warrendale, PA, ISBN 0-7680-0443-8, 1999.

16. Sims-Williams, D.B. and Dominy, R., "Experimental Investigation into Unsteadiness and Instability in Passenger Car Aerodynamics," SAE Technical Paper 980391, 1989, doi: 10.4271/980391.

17. Sims-Williams, D.Dominy, R., "The Validation and Application of a 5 Hole Pressure Probe with Tubing Transfer Correction for Time-Accurate Measurements in Unsteady Flows" Second MIRA International Conference on Vehicle Aerodynamics, Coventry, October, 1998.

18. Sims-Williams, D., "Self-Excited Aerodynamic Unsteadiness Associated with Passenger Cars" PhD Thesis, Durham University, 2001

19. Sims-Williams, D.B. and Duncan, B.D., "The Ahmed Model Unsteady Wake: Experimental and Computational Analyses," SAE Technical Paper 2003-01-1315, *SAE Transactions - Journal of Passenger Cars - Mechanical Systems*, 2003, doi:10.4271/2002-01-1315.

20. Konstantinidis, E., Balabani, S.Yianneskis, M., "Conditional Averaging of Piv Plane Wake Data Using a Cross-Correlation Approach" *Experiments in Fluids* 39(1): 38-47, 2005.

CONTACT INFORMATION

Dr David Sims-Williams
Centre for Automotive Research
School of Engineering and Computing Sciences
Durham University
Durham, DH1 3LE
England
d.b.sims-williams@durham.ac.uk

DEFINITIONS/ABBREVIATIONS

A
Model frontal area

B
Backlight angle

B_{eff}
Effective backlight angle

f
Frequency

S
Strouhal number

U
Velocity

W
Model width

CFD
Computational Fluid Dynamics

PIV
Particle Image Velocimetry

RSP
Reattachment Saddle Point

SN
Stable Separation Node

UF
"Unstable" Focus

URN
"Unstable" Reattachment Node

The Engineering Meetings Board has approved this paper for publication. It has successfully completed SAE's peer review process under the supervision of the session organizer. This process requires a minimum of three (3) reviews by industry experts.

ISSN 0148-7191

SAE Customer Service:
Tel: 877-606-7323 (inside USA and Canada)
Tel: 724-776-4970 (outside USA)
Fax: 724-776-0790
Email: CustomerService@sae.org
SAE Web Address: http://www.sae.org
Printed in USA